Applied Physics Letters

Optical properties and symmetry optimization of spectrally (excitonically) uniform site-controlled GaAs pyramidal quantum dots

Cite as: Appl. Phys. Lett. **118**, 073103 (2021); https://doi.org/10.1063/5.0030296
Submitted: 21 September 2020 • Accepted: 03 February 2021 • Published Online: 18 February 2021

Iman Ranjbar Jahromi, Gediminas Juska, Simone Varo, et al.

Applied Physics Letters ARTICLE scitation.org/journal/apl

Optical properties and symmetry optimization of spectrally (excitonically) uniform site-controlled GaAs pyramidal quantum dots

Cite as: Appl. Phys. Lett. **118**, 073103 (2021); doi: 10.1063/5.0030296
Submitted: 21 September 2020 · Accepted: 3 February 2021 ·
Published Online: 18 February 2021

Iman Ranjbar Jahromi,[1] Gediminas Juska,[1,a)] Simone Varo,[1] Francesco Basso Basset,[2] Francesco Salusti,[2] Rinaldo Trotta,[2] Agnieszka Gocalinska,[1] Francesco Mattana,[1] and Emanuele Pelucchi[1]

AFFILIATIONS

[1]Tyndall National Institute, University College Cork, Lee Maltings, Dyke Parade, Cork T12R5CP, Ireland
[2]Department of Physics, Sapienza University of Rome, Piazzale A. Moro 5, I-00185 Rome, Italy

Note: This paper is part of the APL Special Collection on Non-Classical Light Emitters and Single-Photon Detectors.
[a)]**Author to whom correspondence should be addressed:** gediminas.juska@tyndall.ie

ABSTRACT

GaAs quantum dots (QDs) have recently emerged as state-of-the-art semiconductor sources of polarization-entangled photon pairs, however, without site-control capability. In this work, we present a systematic study of epitaxially grown GaAs/$Al_xGa_{1-x}As$ site-controlled pyramidal QDs possessing unrivaled excitonic uniformity in comparison to their InGaAs counterparts or GaAs QDs fabricated by other techniques. We have experimentally and systematically investigated the binding energy of biexcitons, highlighting the importance of the uniformity of all excitonic lines, rather than concentrating solely on the uniformity of the neutral exciton as a typical figure of merit, as it is normally done in the literature. We present optical signatures of GaAs QDs within a range of ∼250 meV with a remarkable uniformity within each individual sample, the ability to excite the biexciton state resonantly, and a systematic study of the fine-structure splitting (FSS) values—features important for polarization entangled photon emission. While, in general, we observe relatively large FSS distribution and associated non-uniformities, we discuss several strategies to suppress the average FSS values to <15 μeV.

Epitaxial semiconductor quantum dots (QDs), although requiring cryogenic temperature operation, are promising candidates for the realization of quantum technology tasks due to their on demand characteristics, their potential for integration into a photonic chip, and their tunable optical properties through and after growth. Real-world applications will require QD-based non-classical light sources to meet a long list of requirements: spectral purity, overall spectral uniformity, brightness, symmetry, pure single-photon emission, to name but a few. Various growth techniques, such as Stranski–Krastanov processes, droplet epitaxy, and the recently developed local droplet etching, mostly relying on molecular beam epitaxy, have been devised.[1] Pure on-demand,[2] indistinguishable,[3,4] entangled,[5,6] and bright[7,8] QD photon sources were reported; however, due to various tradeoffs, none of the reported state-of-the-art QD-based systems can simultaneously satisfy all technological demands. Some of the aspects related to QDs such as site-control or spectral (excitonic pattern) uniformity are very often left untackled as they are hardly compatible with the random nature of most QD systems.

To address these challenges, we have long ago adopted a different QD fabrication approach based on Metal-Organic Vapor Phase Epitaxy (MOVPE) techniques. The QDs are grown on a (111)B GaAs substrate pre-patterned by tetrahedral pyramidal recesses.[9] QD engineering flexibility allowed deterministic control of $In_{0.25}Ga_{0.75}As$ QD composition, size, and aspect-ratio[10]—all reflected in highly uniform spectra, with very often observed high spectral purity, and high density of polarization-entangled photon emitters.[11,12] On the other hand, a characteristic feature—an antibinding biexciton—of all $In_xGa_{1-x}As$ single QDs, as we observed and reported elsewhere,[13] compromises true on-demand entangled photon pair emission under conventional resonant two-photon excitation (TPE), proven as very effective in a number of other (with a binding biexciton) QD systems.[6,14] Also, a remarkable spectral uniformity of the neutral exciton state of large pitch $In_xGa_{1-x}As$ QDs comparable to the state-of-the-art 1.4 meV in

the literature, considering or not other pyramidal systems,[15,16] is largely unmatched by the internal spectral uniformity of individual QDs. For example, in our $In_xGa_{1-x}As$ QDs, the biexciton binding energy ΔE_{XX} fluctuates independently from the excitonic line position within the values of the distribution with a full-width half-maximum ($FWHM_{\Delta Exx}$) of 2.4 meV or more (a summary will be presented in the discussion). Effectively, both the exciton and biexciton uniformity would be of paramount importance in an advanced quantum information device design with multiple sources of entangled photons.[17]

In order to overcome the latter complications of $In_{0.25}Ga_{0.75}As$ QDs and to explore recently highlighted benefits,[1] an approach based on GaAs as a QD material is reported herein. Pure GaAs QDs in AlGaAs barriers can be engineered in the site-controlled pyramidal QD family and, indeed, have historically represented (in just a few avenues, with moderate Al content in the barriers) the first demonstrators for QD signatures in the system.[18,19] Nevertheless, the GaAs QD system, when non-resonantly pumped, showed a complex excitonic pattern, with difficult to pin point excitonic transitions, e.g., the biexciton transition was often buried in manifold excitonic lines. This pushed historically (in the contest of large pitch pyramids) toward the development of InGaAs dots in AlGaAs barriers[20] and (later) to InGaAs dots in GaAs barriers,[21] which showed a reproducible clean excitonic pattern and have since been the systems analyzed in the literature, while keeping GaAs pyramidal dots in the domain of growth model simulation and validation.[9,22] The recently developed GaAs droplet epitaxy-based GaAs dots show similar excitonic patterns when above barrier excitation is exploited but have shown very clear excitonic patterns and short lifetimes when resonantly excited.[23,24] These features, combined with the high structural symmetry of droplet etched dots, have led to the recent demonstrations of on-demand quantum teleportation and entanglement swapping with quantum emitters.[25,26]

In view of these findings, we decided to revamp GaAs pyramidal QDs and explored avenues for their exploitation in quantum information applications.

QDs were grown by MOVPE on (111)B oriented GaAs substrates pre-patterned with either 7.5 or 10 μm pitch tetrahedrons. A general and rather complex QD formation scheme is given in the supplementary material. The key functional layers, which are relevant in the context of this work and which we are concentrating on, are the confinement barriers and the active QD layer (whose thickness is not known with certainty and is given here as nominal growth values only). Based on the barriers' composition and structure, two different approaches have been studied. In the first one, the barriers are composed of 10–100 nm-thick $Al_xGa_{1-x}As$, where the nominal aluminum content has been set between 0.45 and 1, i.e., pure AlAs. In the second one, a superlattice composed of 25 (0.2 nm period) or 50 (0.1 nm period) AlAs/GaAs pairs was grown. A series of 11 samples with different QD nominal thickness and confinement barriers were studied (full sample structures and experimental conditions are given in the supplementary material).

Depending on the nominal QD structure and the confinement barriers, QD-like spectra with very well reproducible characteristic excitonic peaks were observed in the range of ~270 meV, between 1.82 eV (680 nm) and 1.55 eV (800 nm). It is noteworthy that the typically observed spectra are remarkably similar to those observed from GaAs/AlGaAs QDs fabricated by droplet etching[27] and/or droplet epitaxy.[24,28] The exciton (X) and biexciton (XX) transitions were identified unambiguously by fine-structure splitting (FSS) and single-photon cross correlation measurements. Figure 1(a) shows a representative $GaAs/Al_{0.85}Ga_{0.15}As$ QD spectrum obtained under non-resonant excitation. Like in other GaAs QDs, the biexciton here is on a lower energy side with respect to the neutral exciton transition at variance to their $In_{0.25}Ga_{0.75}As$ counterparts, which always possess an antibinding biexciton. We would like to note that one of the most effective structural differences between the two systems is related to the base of the self-limiting profile: the dimensions of its area define the geometry of a QD. As some of us have discussed,[9] the base size of the $Al_xGa_{1-x}As$ changes from ~60 nm for GaAs to ~10 nm for AlAs (the base, which is the confinement barrier material, is the gallium-enriched $Al_xGa_{1-x}As$ alloy region, conventionally referred to as a vertical quantum wire (VQWr)[29]—see the supplementary material for broader description). Modeling suggests that QDs confined by $Al_xGa_{1-x}As$ with the growing Al content not only have smaller lateral dimensions but also will be taller (thicker) at similar nominal thicknesses because a similar QD volume will be distributed on smaller bases. The typical linewidth of the exciton transitions was found to be in the range of 40–120 μeV; however, it was relatively easy to find

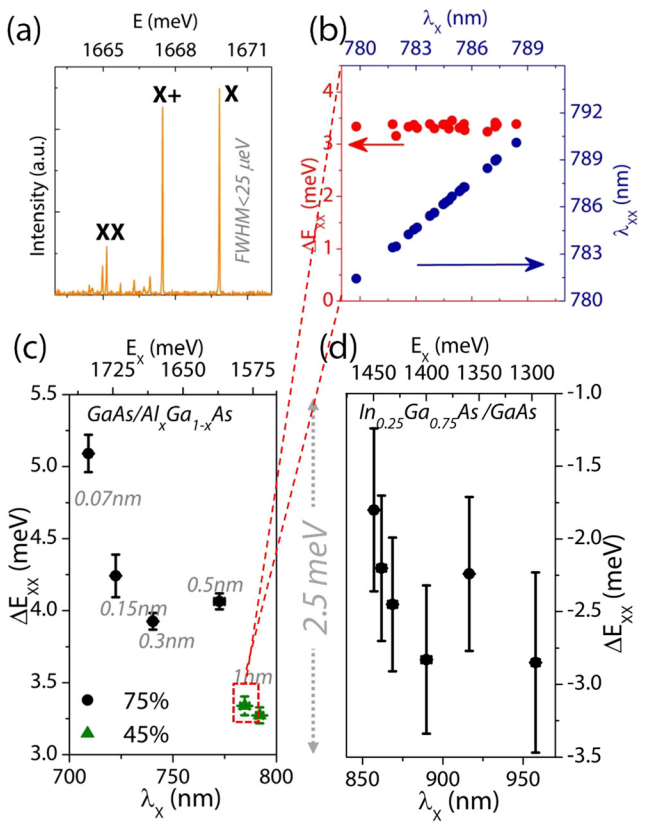

FIG. 1. (a) Spectrum of $GaAs/Al_{0.85}Ga_{0.15}As$ QD with the resolution-limited linewidth below 25 μeV. (b) Biexciton binding energy distribution from individual 1 nm $GaAs/Al_{0.45}Ga_{0.55}As$ QDs. (c) Summary of the biexciton binding energy distribution in $GaAs/Al_{0.45}Ga_{0.55}As$ and $GaAs/Al_{0.75}Ga_{0.25}As$ QDs. Given points are the average values, and the error bars are standard deviations. (d) Summary of the biexciton binding energy distribution in $In_{0.25}Ga_{0.75}As/GaAs$ QDs for comparison. (c) and (d) are shown in the same energy range of 2.5 meV for comparison purposes.

individual QDs with a linewidth, which could not be resolved with our set-up, i.e., <25 μeV [Fig. 1(a)]. One of the main reasons of the linewidth broadening can be largely attributed to the wet-etching processing-induced defects, as we typically see strongly degrading spectra from the pyramids fully released from the supporting substrate.

Figure 1(b) shows the biexciton binding energy ΔE_{XX} distribution as a function of the neutral exciton wavelength λ_x in the QDs with a nominal thickness of 1 nm and confined by $Al_{0.45}Ga_{0.55}As$, which corresponds to $\sim Al_{0.08}Ga_{0.92}As$ composition in the VQWr. In the given case, the full width at half maximum of the ΔE_{XX} normal distribution ($FWHM_{\Delta Exx}$) is 0.15 meV—a spectral shape uniformity that we never observed before. Figure 1(c) summarizes data from several different samples with nominal $Al_{0.75}Ga_{0.25}As$ barriers ($\sim Al_{0.26}Ga_{0.74}As$ in a VQWr). The nominal QD thickness has been within the range of 0.07 and 0.5 nm. While we saw a clear trend of the ΔE_{XX} value ascending with the reduction of the QD size, this did not affect the spectral uniformity we found. A $FWHM_{\Delta Exx}$ as low as 0.107 meV was measured (29 QDs of 0.5 nm nominal thickness used in the statistical calculation). Figure 1(d) represents ΔE_{XX} distribution in $In_{0.25}Ga_{0.75}As/GaAs$ QDs, with $FWHM_{\Delta Exx}$ values in the range of 1.08–1.46 meV. Both distribution graphs show the range of 2.5 meV to highlight an obvious difference of the uniformity between the two generations of pyramidal QDs.

While extremely well reproducible spectra have been found in all the range, the uniformity based on the exciton transition energy E_X was found to be superior as well: the smallest full width at half maximum value of the E_X ($FWHM_{\Delta Ex}$) distribution was found to be 2.45 meV (20 randomly selected 0.15 nm GaAs QDs used in the statistical calculation) in comparison to more typical 6.36 meV in the case of large pitch InGaAs QDs (18 $In_{0.25}Ga_{0.75}As$ QDs of 1 nm used).

The characteristic uniform energetic order of the excitonic spectral features, specifically a binding biexciton ($E_X > E_{XX}$), was found to be especially advantageous. A few meV binding energy ($\Delta E_{XX} = E_X - E_{XX}$) allowed a relatively easy implementation of a resonant two-photon excitation of the biexciton state. The spectrum of a representative $GaAs/Al_{0.45}Ga_{0.55}As$ QD under non-resonant continuous-wave 633 nm excitation is shown in the top graph of Fig. 2(a). The presence of other transitions than the exciton and biexciton and a typically low intensity of the biexciton line are strong drawbacks degrading the performance of a deterministic entangled photon source. Under resonant TPE excitation [Fig. 2(a), bottom graph], the QD is effectively coherently addressed, resulting in an emission originating mostly from the biexciton recombination cascade. A low intensity transition close to XX is attributed to one of the charged complexes—as a result of a random QD charging from the vicinity. The coherent nature of the excitation process is well represented by Rabi oscillations of both, the exciton and biexciton, up to a pulse area of 7π [Fig. 2(b)]. Figure 2(c) shows an autocorrelation curve of the X transition. The calculated $g^{(2)}(0)$ value of 0.028 ± 0.003 (± 3 ns range) confirms single photon emission. Figure 2(d) shows the obtained lifetime decays of the exciton and biexciton. The XX lifetime was found to be 220 ps. The X kinetics was found to be more complicated—a biexponential decay with the lifetime constants of 490 ps and 2 ns. Similarly, slow recombination dynamics related to the effects of a solid-state environment that resemble a well-known QD blinking mechanism has been observed from GaAs QDs.[30] While the origin of the slow decay is not clear and cannot be explained at this stage by a simple on/off QD blinking model,

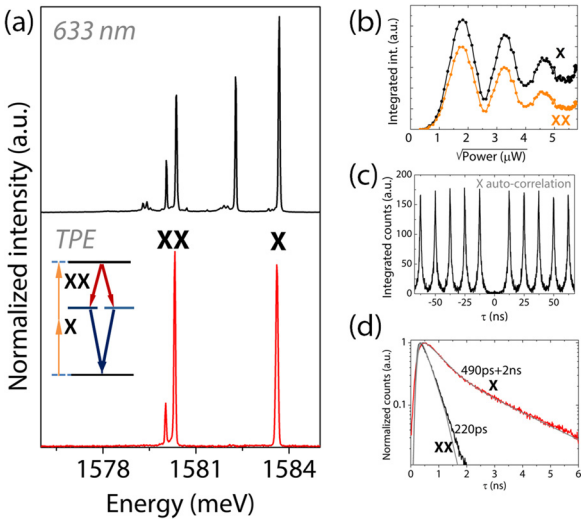

FIG. 2. The resonant TPE of the biexciton. (a) Spectra of a $GaAs/Al_{0.45}Ga_{0.55}As$ QD under non-resonant (top) and resonant (bottom) excitation. (b) Rabi oscillations. (c) An auto-correlation curve demonstrating single photon emission with $g^{(2)}(0) = 0.028 \pm 0.003$ (± 3 ns range). (d) The lifetime decays of the exciton and biexciton.

we would like to stress that the presented results nicely serve as a-proof-of-principle demonstrating the possibility to populate the biexciton state by the resonant TPE and overcome issues arising in the counterpart $In_{0.25}Ga_{0.75}As$ QDs due to an antibinding biexciton.

We must note that the efficiency and the recombination dynamics of the TPE process strongly depend on the vicinity of a QD. Several scenarios have been observed. First, the TPE process can be effectively suppressed in QDs, which tend to be charged due to non-intentional background doping. Such QDs, on the other hand, can be efficiently populated to a trion state with a laser tuned to its excited state. The second type of TPE complication is induced by the excitation laser. Due to the presence of shallow states in the bandgap of the confinement barrier material, the laser, even though tuned to a TPE resonance, can create free charge carriers available to populate a QD after the QD is initialized to the biexciton state. In this case, next to non-intense X and XX transitions, bright peaks of a positively charged biexciton (XX+) are observed. Interestingly, XX+ peaks show Rabi oscillations as well; however, the presence of these oscillations merely presents the fact that the QD is coherently populated to the biexciton state and then, subsequently, is transformed to XX+ through the capture of a hole. Finally, even in the case of an efficient resonant excitation-recombination case, we often observe reduced intensity of the XX state in comparison to X—a deviation from an ideally expected equality of two events bearing in a single recombination cascade. Figure 2(b) is a characteristic representation of such a case. We attribute this to the biexciton dissociation event, such as electron-hole pair depletion within the lifetime of the XX state, rather than to an incoherent X excitation. The intensity difference between X and XX transitions clearly shows pronounced Rabi oscillations matching the ones of the XX transition, suggesting that the excess X radiative recombination events are related to the coherent XX TPE process and not to any sort of incoherent excitation, as for example, we previously observed in

InGaAs QDs with an antibinding biexciton.[13] In the given example in Fig. 2(b), the estimated efficiency of the TPE process by π area pulses and based on the X transition is 0.94; however, due to the XX state dissociation, the XX population estimated from the actual radiative recombination is 0.7.

In either excitation-recombination scenario, to have high efficiency of entangled photon emission, control of these TPE blocking mechanisms will be of paramount importance. To demonstrate an actual possibility for polarization-entangled photon emission, in general, we have added data to the supplementary material (Fig. S4) showing polarization-entangled photon emission from a different sample under non-resonant excitation conditions. As we discuss below, the QD symmetry optimization approaches are essential to ensure high quality of entanglement.

The resonant TPE scheme was effective in a majority of tested QDs from the specific studied sample; however, in none of the cases, we could measure polarization entanglement between the biexciton and exciton due to the non-vanishing fine-structure splitting (FSS). The representative QD shown in Fig. 2 had the FSS equal to 14 μeV, and the overall distribution from this GaAs/$Al_{0.45}Ga_{0.55}$As sample was found to be 60 $\pm$ 38 μeV, with, in general, no specific crystallographic orientation as expected, but often also affected by local sample area features (these being processing related or other and cannot be discussed here). Such a broad distribution of large FSS values is in contradiction with the generally accepted picture of (111) oriented QDs as intrinsically highly symmetric.[31] By several different QD fabrication approaches, it was demonstrated that (111) oriented QDs indeed have smaller FSS values[12,28,32] than conventional Stranski-Krastanov QDs, but they rarely all have sufficiently small FSS values for an efficient bright entangled photon emission. For example, our state-of the-art result, samples with an average exciton FSS equal to ~3 μeV, can be recreated only in a narrow energy range of ~25 meV.[11] Several internal and external perturbations are possibly affecting the symmetry of carrier confinement potential. Among the most effective ones that were theoretically and experimentally identified are the ones related to alloy disorder effects, either internally to a QD or indirectly from the confinement barrier material[33] (e.g., the VQWr disorder in our case). To test how $Al_xGa_{1-x}As$ barriers and QD structural properties affect the FSS, we have developed several QD design strategies. Most relevant results are summarized in Fig. 3.

First, a series of samples with different aluminum contents ($0.45 \leq x \leq 1$) in the barriers was prepared. We observed a general FSS reduction trend with increasing Al content. QDs with pure AlAs confinement barriers (only 10 nm thick in these samples on top of an AlGaAs barrier) had the smallest FSS with an average value of 11 $\pm$ 8 μeV—a reduction that we attribute to the reduced alloy disorder effects. Indeed, in AlAs barriers, alloy disorder should be absent; thus, the residual FSS is most likely caused by a different phenomenon, while we cannot exclude that thicker AlAs layers would help more. It is also highly possible that small structural asymmetries are more effective due to a smaller QD base. However, without the QD morphological characterization, this statement is speculative at this stage.

Second, we systematically altered a QD thickness (nominally 0.035–0.5 nm) confined by $Al_{0.75}Ga_{0.25}$As barriers (~$Al_{0.26}Ga_{0.74}$As in a VQWr). We observed the FSS and its distribution reduction trend within thinner QDs (Fig. 3). QDs with a nominal thickness of 0.07 nm were characterized by an average FSS of 14 $\pm$ 10 μeV. A very similar

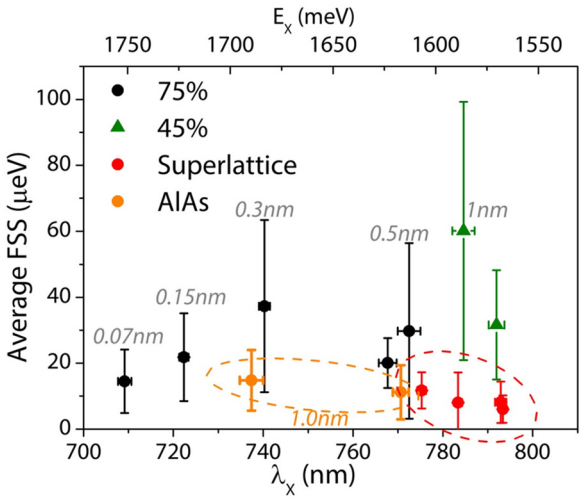

FIG. 3. Average fine-structure splitting of GaAs QDs with different designs: nominal thickness and/or confinement barrier type. See Fig. S2 and tables with the summary of the full epitaxial structure in the supplementary material. Percentages in the legend refer to the AlGaAs nominal barrier Al content.

trend has been observed within the $In_{0.25}Ga_{0.75}$As QD counterparts, where the most symmetric QDs were the thinnest with the ground states approaching the top of the confinement barriers.[11] Carrier wavefunctions' leakage to the barriers, which reduces electron-hole exchange interaction and thus fine-structure splitting,[34] could explain the observed FSS reduction trends. We do not show results from the thinnest 0.035 nm QDs as we could not identify X and XX transitions due to a very weak or absent intensity of the biexciton and actually a small FSS of all the observed peaks.

Finally, we adopted a third, and the most promising, strategy—a QD confinement by GaAs/AlAs superlattices. 20 periods of nominal 0.1 or 0.2 nm thickness were grown on both sides of a QD. The aim of introducing a digital alloy superlattice was to minimize alloy disorder effects (without expecting any zeroing obviously in view of always present interface disorder effects) occurring within the conventional $Al_xGa_{1-x}As$. Such a digital alloy superlattice of GaAs/AlAs is expected to act as an effective $Al_{0.5}Ga_{0.5}$As barrier providing confinement for a QD, however, without alloy disorder effects. By introducing this design, we systematically could reduce the FSS values below 15 μeV, with the best average value of 6 $\pm$ 4 μeV in QDs with 0.85 nm as nominal thickness (polarization entanglement data obtained under non-resonant excitation conditions from one of the QDs of this sample are shown in the supplementary material).

In summary, we have presented a design and systematic study of GaAs site-controlled pyramidal QDs possesing properties highly promising for advanced quantum optics applications. A remarkable state-of-the-art spectral (excitonic pattern) uniformity between individual QDs has been demonstrated as a signature of the overall morphological uniformity. The characteristic feature, a binding biexciton, of all GaAs QDs was found to be advantegous to overcome complications related to an antibinding biexciton in the counterpart $In_{0.25}Ga_{0.75}$As QDs for resonant two-photon excitation of the biexciton state. Such TPE ability has been demonstrated. We presented

several routes to minimize the fine-structure splitting in the QDs. The approach based on a Ga/Al digital alloy superlattice as the confinement barrier was found to be the most promising one even if more work is needed to further reduce the residual FSS.

AUTHORS' CONTRIBUTIONS

I.R.J. and G.J. contributed equally.

See the supplementary material for the epitaxial structures and fabrication methods of all samples and polarization-resolved optical measurements of the fine-structure splitting and polarization-entanglement.

This research was supported by Science Foundation Ireland under Grant Nos. 15/IA/2864, 12/RC/2276_P2, and SFI-18/SIRG/5526; and by the European Research Council (ERC) under the European Union's Horizon 2020 Research and Innovation Programme (SPQRel, Grant Agreement No. 679183).

DATA AVAILABILITY

The data that support the findings of this study are available from the corresponding author upon reasonable request.

REFERENCES

[1]M. Gurioli, Z. Wang, A. Rastelli, T. Kuroda, and S. Sanguinetti, "Droplet epitaxy of semiconductor nanostructures for quantum photonic devices," Nat. Mater. **18**, 799–810 (2019).
[2]P. Michler, A. Kiraz, C. Becher, W. V. Schoenfeld, P. M. Petroff, L. Zhang, E. Hu, and A. Imamoglu, "A quantum dot single-photon turnstile device," Science **290**, 2282–2285 (2000).
[3]C. Santori, D. Fattal, J. Vučković, G. S. Solomon, and Y. Yamamoto, "Indistinguishable photons from a single-photon device," Nature **419**, 594–597 (2002).
[4]E. Schöll, L. Hanschke, L. Schweickert, K. D. Zeuner, M. Reindl, S. F. Covre da Silva, T. Lettner, R. Trotta, J. J. Finley, K. Müller, A. Rastelli, V. Zwiller, and K. D. Jöns, "Resonance fluorescence of GaAs quantum dots with near-unity photon indistinguishability," Nano Lett. **19**(4), 2404–2410 (2019).
[5]N. Akopian, N. H. Lindner, E. Poem, Y. Berlatzky, J. Avron, D. Gershoni, B. D. Gerardot, and P. M. Petroff, "Entangled photon pairs from semiconductor quantum dots," Phys. Rev. Lett. **96**, 130501 (2006).
[6]D. Huber, M. Reindl, S. F. Covre da Silva, C. Schimpf, J. Martín-Sánchez, H. Huang, G. Piredda, J. Edlinger, A. Rastelli, and R. Trotta, "Strain-Tunable GaAs Quantum Dot: A Nearly Dephasing-Free Source of Entangled Photon Pairs on Demand," Phys. Rev. Lett. **121**, 033902 (2018).
[7]J. Liu, R. Su, Y. Wei, B. Yao, S. F. Covre da Silva, Y. Yu, J. Iles-Smith, K. Srinivasan, A. Rastelli, J. Li, and X. Wang, "A solid-state source of strongly entangled photon pairs with high brightness and indistinguishability," Nat. Nanotechnol. **14**, 586 (2019).
[8]H. Wang, H. Hu, T.-H. Chung, J. Qin, X. Yang, J.-P. Li, R.-Z. Liu, H.-S. Zhong, Y.-M. He, X. Ding, Q. Deng, Y.-H. Dai, Y.-H. Huo, S. Höfling, C.-Y. Lu, and J.-W. Pan, "On-demand semiconductor source of entangled photons which simultaneously has high fidelity, efficiency, and indistinguishability," Phys. Rev. Lett. **122**, 113602 (2019).
[9]V. Dimastrodonato, E. Pelucchi, and D. D. Vvedensky, "Self-limiting evolution of seeded quantum wires and dots on patterned substrates," Phys. Rev. Lett. **108**, 256102 (2012).
[10]G. Juska, V. Dimastrodonato, L. O. Mereni, T.-H. Chung, A. Gocalinska, E. Pelucchi, B. Van Hattem, M. Ediger, and P. Corfdir, "Complex optical signatures from quantum dot nanostructures and behavior in inverted pyramidal recesses," Phys. Rev. B. **89**, 205430 (2014).
[11]G. Juska, E. Murray, V. Dimastrodonato, T. H. Chung, S. T. Moroni, A. Gocalinska, and E. Pelucchi, "Conditions for entangled photon emission from (111)B site-controlled pyramidal quantum dots," J. Appl. Phys. **117**, 134302 (2015).
[12]G. Juska, V. Dimastrodonato, L. O. Mereni, A. Gocalinska, and E. Pelucchi, "Towards quantum-dot arrays of entangled photon emitters," Nat. Photonics **7**(7), 527–531 (2013).
[13]G. Juska, I. Ranjbar Jahromi, F. Mattana, S. Varo, V. Dimastrodonato, and E. Pelucchi, "Biexciton initialization by two-photon excitation in site-controlled quantum dots: The complexity of the antibinding state case," Appl. Phys. Lett. **117**, 134001 (2020).
[14]M. Müller, S. Bounouar, K. D. Jöns, M. Glässl, and P. Michler, "On-demand generation of indistinguishable polarization-entangled photon pairs," Nat. Photonics **8**, 224–228 (2014).
[15]A. Mohan, P. Gallo, M. Felici, B. Dwir, A. Rudra, J. Faist, and E. Kapon, "Record-low inhomogeneous broadening of site-controlled quantum dots for nanophotonics," Small **6**(12), 1268 (2010).
[16]P. Atkinson, E. Zallo, and O. G. Schmidt, "Independent wavelength and density control of uniform GaAs/AlGaAs quantum dots grown by infilling self-assembled nanoholes," J. Appl. Phys. **112**, 054303 (2012).
[17]M. Reindl, K. D. Jöns, D. Huber, C. Schimpf, Y. Huo, V. Zwiller, A. Rastelli, and R. Trotta, "Phonon-assisted two-photon interference from remote quantum emitters," Nano Lett. **17**, 4090 (2017).
[18]A. Hartmann, Y. Ducommun, L. Loubies, K. Leifer, and E. Kapon, "Structure and photoluminescence of single AlGaAs/GaAs quantum dots grown in inverted tetrahedral pyramids," Appl. Phys. Lett. **73**, 2322 (1998).
[19]A. Hartmann, Y. Ducommun, E. Kapon, U. Hohenester, and E. Molinari, "Few-particle effects in semiconductor quantum dots: Observation of multicharged excitons," Phys. Rev. Lett. **84**, 5648 (2000).
[20]M. H. Baier, S. Watanabe, E. Pelucchi, and E. Kapon, "High uniformity of site-controlled pyramidal quantum dots grown on prepatterned substrates," Appl. Phys. Lett. **84**, 1943 (2004).
[21]L. O. Mereni, V. Dimastrodonato, R. J. Young, and E. Pelucchi, "A site-controlled quantum dot system offering both high uniformity and spectral purity," Appl. Phys. Lett. **94**, 223121 (2009).
[22]V. Dimastrodonato, E. Pelucchi, P. A. Zestanakis, and D. D. Vvedensky, "Transient and self-limited nanostructures on patterned surfaces," Phys. Rev. B **87**, 205422 (2013).
[23]D. Huber, M. Reindl, Y. Huo, H. Huang, J. S. Wildmann, O. G. Schmidt, A. Rastelli, and R. Trotta, "Highly indistinguishable and strongly entangled photons from symmetric GaAs quantum dots," Nat. Commun. **8**, 15506 (2017).
[24]F. Basso Basset, S. Bietti, M. Reindl, L. Esposito, A. Fedorov, D. Huber, A. Rastelli, E. Bonera, R. Trotta, and S. Sanguinetti, "High-yield fabrication of entangled photon emitters for hybrid quantum networking using high-temperature droplet epitaxy," Nano Lett. **18**(1), 505 (2018).
[25]F. Basso Basset, M. B. Rota, C. Schimpf, D. Tedeschi, K. D. Zeuner, S. F. Covre da Silva, M. Reindl, V. Zwiller, K. D. Jöns, A. Rastelli, and R. Trotta, "Entanglement swapping with photons generated on demand by a quantum dot," Phys. Rev. Lett. **123**, 160501 (2019).
[26]M. Reindl, D. Huber, C. Schimpf, S. F. Covre da Silva, M. B. Rota, H. Huang, V. Zwiller, K. D. Jöns, A. Rastelli, and R. Trotta, "All-photonic quantum teleportation using on-demand solid-state quantum emitters," Sci. Adv. **4**(12), eaau1255 (2018).
[27]A. Küster, Ch. Heyn, A. Ungeheuer, G. Juska, S. T. Moroni, E. Pelucchi, and W. Hansen, "Droplet etching of deep nanoholes for filling with self-aligned complex quantum structures," Nanoscale Res. Lett. **11**, 282 (2016).
[28]T. Kuroda, T. Mano, N. Ha, H. Nakajima, H. Kumano, B. Urbaszek, M. Jo, M. Abbarchi, Y. Sakuma, K. Sakoda, I. Suemune, X. Marie, and T. Amand, "Symmetric quantum dots as efficient sources of highly entangled photons: Violation of Bell's inequality without spectral and temporal filtering," Phys. Rev. B **88**, 041306(R) (2013).
[29]Q. Zhu, E. Pelucchi, S. Dalessi, K. Leifer, M.-A. Dupertuis, and E. Kapon, "Alloy segregation, quantum confinement, and carrier capture in self-ordered pyramidal quantum wires," Nano Lett. **6**(5), 1036–1041 (2006).
[30]J.-P. Jahn, M. Munsch, L. Béguin, A. V. Kuhlmann, M. Renggli, Y. Huo, F. Ding, R. Trotta, M. Reindl, O. G. Schmidt, A. Rastelli, P. Treutlein, and R. J. Warburton, "An artificial Rb atom in a semiconductor with lifetime-limited linewidth," Phys. Rev. B **92**, 245439 (2015).

[31]A. Schliwa, M. Winkelnkemper, A. Lochmann, E. Stock, and D. Bimberg, "In(Ga)As/GaAs quantum dots grown on a (111) surface as ideal sources of entangled photon pairs," Phys. Rev. B **80**, 161307 (2009).
[32]M. A. M. Versteegh, M. E. Reimer, K. D. Jöns, D. Dalacu, P. J. Poole, A. Gulinatti, A. Giudice, and V. Zwiller, "Observation of strongly entangled photon pairs from a nanowire quantum dot," Nat. Commun. **5**, 5298 (2014).
[33]V. Mlinar and A. Zunger, "Effect of atomic-scale randomness on the optical polarization of semiconductor quantum dots," Phys. Rev. B **79**, 115416 (2009).
[34]M. Bayer, G. Ortner, O. Stern, A. Kuther, A. A. Gorbunov, A. Forchel, P. Hawrylak, S. Fafard, K. Hinzer, T. L. Reinecke, S. N. Walck, J. P. Reithmaier, F. Klopf, and F. Schäfer, "Fine structure of neutral and charged excitons in self-assembled In(Ga)As/(Al)GaAs quantum dots," Phys. Rev. B **65**, 195315 (2002).